INTERNATIONAL JOURNAL FOR NUMERICAL METHODS IN FLUIDS
Int. J. Numer. Meth. Fluids 2006; **52**:1159–1174
Published online 7 April 2006 in Wiley InterScience (www.interscience.wiley.com). DOI: 10.1002/fld.1226

Application of the TVD scheme to the nonlinear instability analysis of a capillary jet

Stephen G. Chuech[1,*,†] and Ming-Ming Yan[2,‡]

[1]*Department of Mechanical and Mechatronic Engineering, National Taiwan Ocean University, Keelung 202, Taiwan*
[2]*Chung-Shan Institute of Science and Technology, PO Box 90008-17-10, Lung-Tan, Tao-Yuan 325, Taiwan*

SUMMARY

In the past, when either the perturbation-type method or direct-simulation approach was used to analyse capillary jets, the governing equations, which are parabolic in time and elliptic in space, were simplified or linearized. In the present study, the convective derivative term and a full, nonlinear form of the capillary pressure term are retained in the governing equations to investigate nonlinear effects on the break-up of capillary jets. In this work, the TVD (i.e. total variation diminishing) scheme with flux-vector splitting is applied to obtain the solutions of the system of nonlinear equations in a matrix form. Numerical results show that the present nonlinear model predicts longer jet break-up lengths and slower growth rates for capillary jets than the previous linear model does. Comparing with other measurements from past literatures, the nonlinear results are consistent with the experimental data and appear more accurate than the linear analysis. In the past, the classic perturbation-type analyses assumed constant growth rates for the fundamental and all harmonic components. By contrast, the present model is able to capture the local features of growth rates, which are not spatially and temporally constant. Copyright © 2006 John Wiley & Sons, Ltd.

KEY WORDS: TVD scheme; capillary jet; jet break-up; growth rates; satellite drop

1. INTRODUCTION

An understanding of the liquid jet break-up process is of vital importance in the design of many practical devices such as internal engine combustors [1, 2], gas turbines [3], liquid rocket engines [4], and MEMS ejectors [5–7]. Applications for the capillary jet break-up range from ink jet printing to drug delivery systems [5–7]. In ink jet printing, a capillary jet is ejected

*Correspondence to: Stephen G. Chuech, Department of Mechanical and Mechatronic Engineering, National Taiwan Ocean University, Keelung 20224, Taiwan.
†E-mail: sgc@mail.ntou.edu.tw
‡E-mail: yanmm@ms32.hinet.net

Received 25 September 2005
Revised 9 January 2006
Accepted 16 February 2006

to produce small drops, which are often accompanied by satellite drops. The appearance of satellite drops during the jet break-up process may result in print quality defects; therefore, the issue of the capillary jet break-up still demands much attention.

Although the investigation of nonlinear effects on the jet break-up is critical to understand the occurrence of satellite drops, previous studies [8–13] still utilized the linear instability analysis by neglecting the convective derivative term in the momentum equation due to the nonlinear complexity involved in the governing equations. In these linear analyses, only the fundamental mode was considered and its growth rate was assumed to be constant. In fact, the existence of harmonic modes other than the fundamental can be inferred from the observation [14] that capillary jets do not break up into mono-size droplets, as the linear theory would suggest.

Therefore, several studies, including perturbation-type analyses [15–18] and direct-simulation models [19–27], preserved the convective derivative term to deal with the nonlinear temporal instability. However, in the category of the perturbation type, their analyses [15–18] retained only the first few harmonics in the perturbation expansions where the wave growth rate was still assumed to be a constant of time. In the category of direct methods, the one-dimensional models [19, 20] also utilized the expansion technique to simplify the computational procedure. Lee [19] applied the Lax–Wendroff method to the PDE for numerical solutions in which the Taylor expansion was approximated only to the second-order time step. Similarly, in Torpey's approach [20], the formation of satellite drops was considered as a function of the amplitude of the secondary harmonic because the third and higher harmonics were neglected. Other direct simulations [21–27] circumvented the numerical difficulties through linearization of the highly nonlinear capillary pressure term. The full capillary pressure term, which does affect the satellite drop formation, should not be simplified.

Although a full nonlinear transient Navier–Stokes system for the dynamics of drop formation was recently solved in two dimensions by Wilkes *et al.* [28], algorithms for obtaining accurate solutions of the two-dimensional equations were computationally intensive due to the required small time steps and fine grids across the entire jet and interface. Ambravaneswaran *et al.* [29] remarked that one-dimensional models indeed hold certain advantages over their two-dimensional counterparts, in terms often of both programming efforts and computational time. Especially, it is questionable to immediately utilize the two-dimensional solutions to obtain the jet break-up length. On the other hand, it should be noticed that all the one- or two-dimensional analyses mentioned above focused only on the formation of main and satellite drops but reported no information of the jet break-up length and the growth rates of disturbances on the jet surface.

Therefore, in this article, a one-dimensional system is adopted to study the instability and break-up of capillary jets. In the governing equations, the convective derivative term and the capillary pressure term in its full form are included to preserve all aspects of nonlinear nature. The equations in a matrix form, which are parabolic in time and elliptic in space, will be solved by a TVD upwind scheme with flux-vector splitting [30]. Meanwhile, the predictions for the jet break-up length and the wave growth rate are emphasized in this study. For a validation of the present model, various experimental cases of Grant and Middleman [31] will be simulated and compared for the jet break-up lengths. For a further comparison, the local wave growth rates predicted by the present model are averaged to compare with the linear solutions of Rayleigh [8] and experimental data of

Donnely and Glaberson [32] though they should not be spatially and temporally constant. The comparison results show that the nonlinear solutions for the break-up length and wave growth rate are basically in agreement with the measurements. The nonlinear model predicts longer break-up lengths and lower growth rates than the linear theory does.

2. GOVERNING EQUATIONS

One-dimensional study indeed holds advantages of large savings in programming and computational time. Therefore, the present paper adopts a one-dimensional model with the assumption of plug jet velocity profile to study the instability and break-up of a capillary jet, as shown in Figure 1. The present study is an application of the TVD scheme to the capillary jet break-up. One of main objectives of the article concerns whether the TVD scheme may handle the flux-splitting phenomenon appearing inside the jet thread during the break-up process. Therefore, liquid viscosity and gravity were neglected for the study to facilitate the analysis of the TVD scheme. In the model, it was assumed that the effects of turbulence, cavitation, velocity profile, relaxation, and helical and Kelvin–Helmholtz instabilities played no role, so that only the capillary instability appeared in the break-up process. The model also considered the capillary jet as an infinitely long cylinder without the aerodynamic effects of ambient air. The liquid jet was assumed to be stationary relative to a moving observer. Thus, when the jet is initially at rest to be perturbed by an infinitesimal sinusoidal disturbance, the transient motion of inviscid liquid will be governed by the following continuity and momentum equations:

$$\frac{1}{r}\frac{\partial}{\partial r}(ru_r)+\frac{\partial}{\partial z}(u_z)=0 \tag{1}$$

$$\frac{\partial}{\partial t}(u_z)+\frac{1}{r}\frac{\partial}{\partial r}(ru_zu_r)+\frac{\partial}{\partial z}(u_z^2)=-\frac{1}{\rho}\frac{\partial p}{\partial z} \tag{2}$$

where u_z and u_r represent the axial and radial perturbation velocities, respectively, ρ is liquid density, and p is the perturbation pressure.

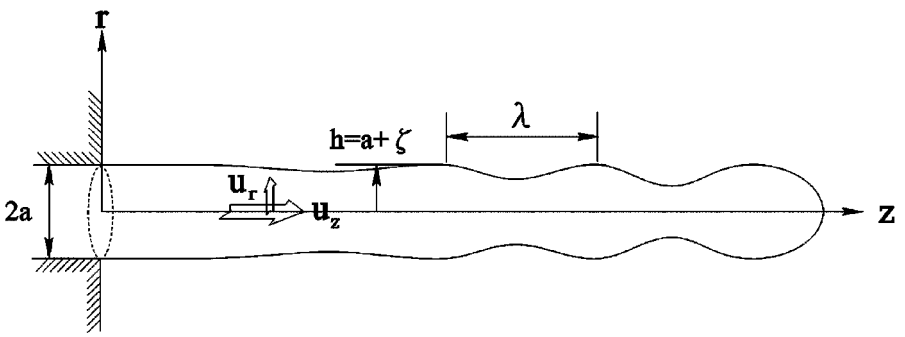

Figure 1. Unstable disturbances growing on the surface of a capillary jet.

By integrating Equations (1) and (2) with respect to r from the jet centreline to the jet interface, the equations become

$$hu_r + \frac{h^2}{2}\frac{\partial}{\partial z}(u_z) = 0 \tag{3}$$

$$\frac{h^2}{2}\frac{\partial}{\partial t}(u_z) + hu_z u_r + \frac{h^2}{2}\frac{\partial}{\partial z}(u_z^2) = -\frac{h^2}{2\rho}\frac{\partial p}{\partial z} \tag{4}$$

where h is the local jet radius $h = a + \zeta$; a and ζ denote the radius of the capillary tube and the local amplitude of the growing disturbance on the jet surface, respectively. At the interface, ζ is essentially the interfacial displacement function of t and z, and the radial velocity u_r should be equal to the total derivative of the $\zeta(t,z)$. Therefore, the relationship between the radial and axial velocities can be related to the local jet radius:

$$u_r = \frac{\partial h}{\partial t} + u_z\frac{\partial h}{\partial z} \tag{5}$$

Substituting Equation (5) into Equations (3) and (4), the equations [25] become

$$\frac{\partial}{\partial t}(h^2) + \frac{\partial}{\partial z}(h^2 u_z) = 0 \tag{6}$$

$$\frac{\partial}{\partial t}(h^2 u_z) + \frac{\partial}{\partial z}(h^2 u_z^2) = -\frac{h^2}{\rho}\frac{\partial p}{\partial z} \tag{7}$$

$$p = p_\sigma = \sigma\left\{\frac{1}{h}\left[1 + \left(\frac{\partial h}{\partial z}\right)^2\right]^{-1/2} - \frac{\partial^2 h}{\partial z^2}\left[1 + \left(\frac{\partial h}{\partial z}\right)^2\right]^{-3/2}\right\} \tag{8}$$

Owing to surface tension σ involved in the interfacial equilibrium for the capillary jet, the pressure p should balance with the capillary pressure p_σ [25, 33]. The first term on the right-hand side of Equation (8) is a destabilizing source, which results in the necking process and leads to the satellite drop formation. On the other hand, the second term in Equation (8) is a stabilizing source and always induces a restoring force.

3. NUMERICAL METHOD

To facilitate the analysis, Equations (6) and (7) are expressed in dimensionless form as follows:

$$\frac{\partial \tilde{r}}{\partial T} + \frac{\partial \tilde{v}}{\partial Z} = 0 \tag{9}$$

$$\frac{\partial \tilde{v}}{\partial T} + \frac{\partial}{\partial Z}(\tilde{v}^2/\tilde{r}) = -\tilde{r}\frac{\partial}{\partial Z}(\tilde{R}_1^{-1} + \tilde{R}_2^{-1}) \tag{10}$$

where dimensionless time $T = t/\sqrt{\rho a^3/\sigma}$ and dimensionless axial coordinate $Z = z/a$. The variables appearing in Equations (9) and (10) are dimensionless groups: $\tilde{r} = (h/a)^2 = H^2$,

$\tilde{v} = u_z h^2 \sqrt{\rho/\sigma a^3}$, and $\tilde{R}_1$ and $\tilde{R}_2$ are mutually orthogonal principal radii of curvature of the jet surface in dimensionless form:

$$\tilde{R}_1 = H\left[1 + \left(\frac{\partial H}{\partial Z}\right)^2\right]^{1/2} \tag{11}$$

$$\tilde{R}_2 = -\left(\frac{\partial^2 H}{\partial Z^2}\right)^{-1}\left[1 + \left(\frac{\partial H}{\partial Z}\right)^2\right]^{3/2} \tag{12}$$

Furthermore, Equations (9) and (10) can be written in a matrix form as:

$$\frac{\partial G}{\partial T} + \frac{\partial E}{\partial Z} = S \tag{13}$$

where

$$G = \begin{bmatrix} \tilde{r} \\ \tilde{v} \end{bmatrix} \tag{14}$$

$$E = \begin{bmatrix} \tilde{v} \\ \tilde{v}^2/\tilde{r} \end{bmatrix} \tag{15}$$

$$S = \begin{bmatrix} 0 \\ \tilde{s} \end{bmatrix} \tag{16}$$

The capillary term in its full form in Equations (10)–(12) was treated as a source term $\tilde{s}$ for the matrix system and no curve fitting was used during the whole computation. A TVD upwind scheme with flux-vector splitting [30] was used to solve Equation (13). In the TVD scheme, the flux-vector E may be expressed directly in terms of its Jacobian A as $E = AG$. Note that A is the Jacobian with respect to $\tilde{r}$ and $\tilde{v}$. Thus, we can split the flux-vector into two parts:

$$E^+ = \frac{(A + |A|)}{2} G \tag{17}$$

$$E^- = \frac{(A - |A|)}{2} G \tag{18}$$

where $|A| = M|\Lambda|M^{-1}$, $|\Lambda|$ is a diagonal matrix with absolute eigenvalues of A, and M^{-1} is an inverse of the matrix M which diagonalizes A. Hence, Equation (13) can now be written as

$$\frac{\partial G}{\partial T} + \frac{\partial E^+}{\partial Z} + \frac{\partial E^-}{\partial Z} = S \tag{19}$$

Moreover, the equation can be rewritten in finite-difference form as

$$G_i^{k+1} = G_i^k - \psi\left[E^k_{i+\frac{1}{2}} - E^k_{i-\frac{1}{2}}\right] + S_i^k \cdot \Delta T \tag{20}$$

where $\Delta T = (T^{k+1} - T^k)$, $\psi = (T^{k+1} - T^k)/(Z_{i+(1/2)} - Z_{i-(1/2)})$, and a numerical flux function is introduced and defined as follows:

$$E_{i-(1/2)} = \tfrac{1}{2}[A(G_i + G_{i-1})] - \tfrac{1}{2}|A|[G_i - G_{i-1}] \tag{21}$$

4. BOUNDARY AND INITIAL CONDITIONS

In the numerical computation, the disturbance wavelength λ was taken as a computational domain for a given dimensionless wavenumber, $K = 2\pi a/\lambda$. The boundaries at the right and left ends of this one-dimensional computational domain were prescribed with periodicity. In other words, the calculation field was kept fixed over one wavelength with cyclic boundary conditions. This is the feature of a standing wave for which the coordinate is moving with the jet velocity as assumed previously. As a result, spatially periodic contracting and bulging on the jet surface are developing with time marching. Initially, the local jet radius along the z-axis direction at $T = 0$ can be expressed in dimensionless form as

$$h = \zeta_0 \cdot \cos(kz) + a \tag{22}$$

where k is the wavenumber and ζ_0 is the initial amplitude. Since the system is initially at rest, the velocity is zero over the whole flow field at $T = 0$. Once the axisymmetric sinusoidal disturbance is imposed on the jet surface, the curvature of the wave profile will induce a capillary force to initiate the flow motion.

The dependent variables were solved through the Equations (13)–(21) with the boundary and initial conditions mentioned above. A uniform one-dimensional grid system was adopted for all computations. For the grid system, 50 computational cells were used for most cases while a 100-cell grid system was employed for some cases of dimensionless wavenumber K close to zero or one due to small growth rates or necessary resolutions for tiny satellites. In order to avoid numerical instability, the step sizes of time marching were limited to 5% of the quotient of the grid size divided by the characteristic velocity.

5. DROP FORMATION

The linear instability theory [8] shows that the cut-off dimensionless wavenumber is always one for the capillary jet. In other words, when K is greater than one, the second term of the capillary pressure in Equation (8) is a stabilizing source and will induce a restoring force. As a result, the initial disturbance wave decays with time and the jet surface will eventually restore to the originally undisturbed position. In order to simulate the surface wave evolution and drop formation of an unstable jet in the break-up process, the value of K less than one should be selected.

According to the linear theory, solutions of the dispersion relation providing the maximum growth rate correspond to a value of the dimensionless wavenumber K approximately equal to 0.7. Therefore, the most unstable jet, perturbed at $K = 0.7$, was first simulated for the evolution in time of the jet surface wave. The flow conditions for the experimental cases of Rutland and Jameson [14] were adopted similar to the present test conditions. Figure 2 indicates that the growth of the disturbance wave on the perturbed jet surface is not significant at the early

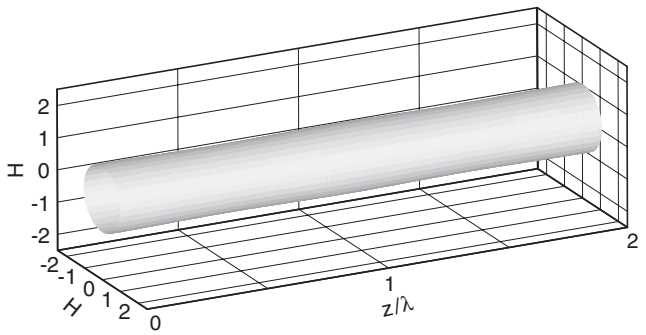

Figure 2. Wave profile on the jet surface for $K = 0.7$ at $T = 3.57$.

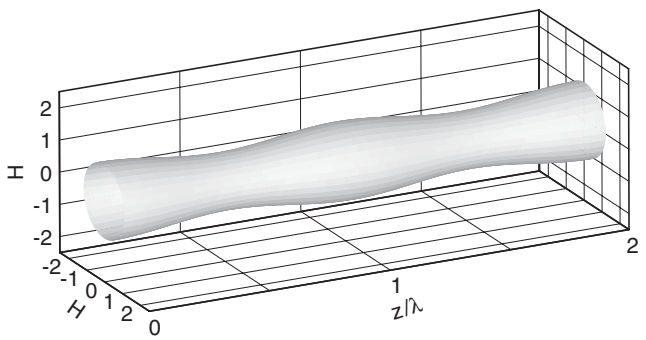

Figure 3. Wave profile on the jet surface for $K = 0.7$ at $T = 10.28$.

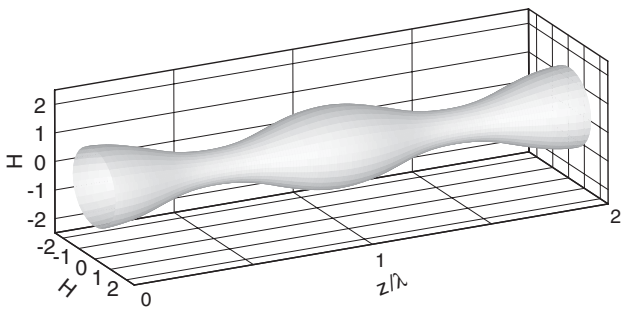

Figure 4. Wave profile on the jet surface for $K = 0.7$ at $T = 13.05$.

stage of $T = 3.57$. The results in Figures 3 and 4 show that a neck gradually forms at the trough position and the trough contracts at a faster rate than the swell grows from $T = 10.28$ to 13.05. This phenomenon gives evidence that the wave growth rate is not constant spatially and temporally. Figure 5 shows that the jet is about to disintegrate at $T = 15.47$. From Figure 5,

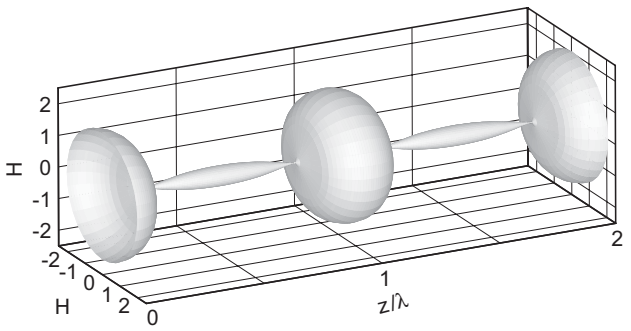

Figure 5. Formation of main and satellite drops before the jet break-up for $K = 0.7$ at $T = 15.47$.

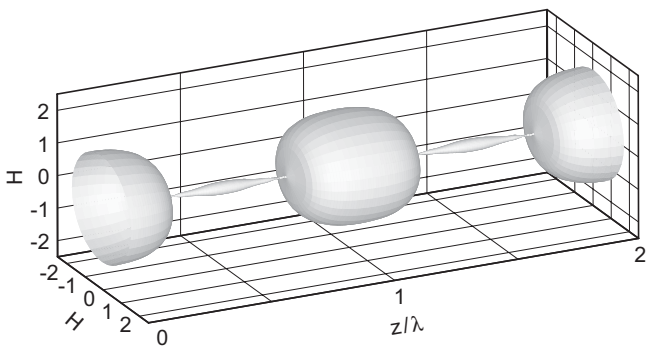

Figure 6. Formation of main and satellite drops before the jet break-up for $K = 0.9$ at $T = 18.67$.

it can be seen that as soon as the jet surfaces at two ends of the slender neck touch the centreline, the swell portions will become main drops and the neck will turn into a satellite drop in between at the trough position.

The evolution profiles of the jet surface wave can be further demonstrated by the cases of $K = 0.9$ and 0.3, as shown in Figures 6 and 7. Figure 6 shows the wave profile for $K = 0.9$ just before the jet break-up at $T = 18.67$. Comparing to the case of $K = 0.7$, the trough still contracts faster than the swell grows, but the slender neck becomes shorter to form a smaller satellite drop due to the short wavelength of $K = 0.9$. It is obvious that the case of $K = 0.9$ takes longer to break up because the disturbance wave of $K = 0.7$ grows at the fastest rate according to the linear analysis.

For the case of $K = 0.3$, where the disturbance possesses a relatively long wavelength, the trough contracts at a slower rate than the swell grows, and eventually produces a relatively large satellite drop, as shown in Figure 7. This phenomenon is contrary to the cases of $K = 0.7$ and 0.9 with relatively short wavelengths. From Figures 5–7, it can be observed that the size of satellite drop is basically smaller than that of main drop in the break-up process. However, the size of satellite drop increases with increasing the disturbance wavelength and gradually becomes comparable to that of main drop.

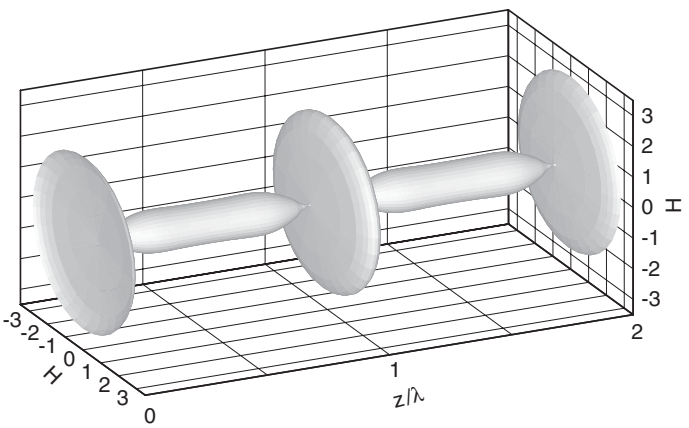

Figure 7. Formation of main and satellite drops before the jet break-up for $K = 0.3$ at $T = 27.18$.

6. JET SHAPE AND BREAK-UP LENGTH

The axisymmetric disturbance of $K < 1$ will exponentially grow and propagate along the flow direction to disintegrate the jet when the amplitude becomes comparable to the undisturbed jet radius. To simulate such a jet shape, a water cylinder of diameter $d = 0.4$ mm, issuing from a nozzle at a velocity of $U = 1.5$ m/s, was first considered for $K = 0.33$, 0.48, 0.6, 0.7, 0.8, and 0.9. During the computations, the evolution of the wave profile was traced and plotted along the jet surface according to flow velocity. It can be seen in Figure 8 that the wave profiles on the jet surface are not significant in the upstream region, but a satellite drop forms at the jet tail. Similar to the results in Figures 5–7, the size of satellite drop is comparable to that of main drop for the case of $K = 0.33$. On the contrary, the satellite drop becomes smaller as the disturbance wavelength decreases. In Figure 8, the jet of $K = 0.7$ exhibits the shortest length owing to its characteristics of the fastest growth.

Rutland and Jameson [34] observed the jet shape using a series of water jets perturbed at various wavenumbers from $K = 0.075$ to 0.683. In the present study, two of their cases (i.e. $K = 0.25$ and 0.683) were simulated and shown in Figure 9. Again, the size of satellite drop is comparable to that of main drop for the long-wavelength case of $K = 0.25$. By contrast, the jet of $K = 0.683$ exhibits a much shorter length and produces relatively smaller drops. The present predicted jet shapes and lengths of $K = 0.25$ and 0.683 are in good agreement with the photographs of Rutland and Jameson [34] in the literature. The only difference is that in the photographs [34] several main and satellite drops, which are separate in space, can be observed beyond the jet tail. The present simulations in Figure 9 were performed only up to the jet disintegration location where the jet surface contracts to touch the centreline.

A value for the continuous length L of the jet prior to break-up is termed 'break-up length'. In describing jet instability, one usually refers to the behaviour of the break-up length as a function of the jet velocity. The break-up length of a liquid jet in a Rayleigh regime can be obtained from the relation $L = Ut$. The linear relationship is reasonably well described by Weber's analysis [9] for the break-up of a laminar Newtonian jet under the influence of surface tension forces alone. According to Weber's theory, the jet is assumed to be subject

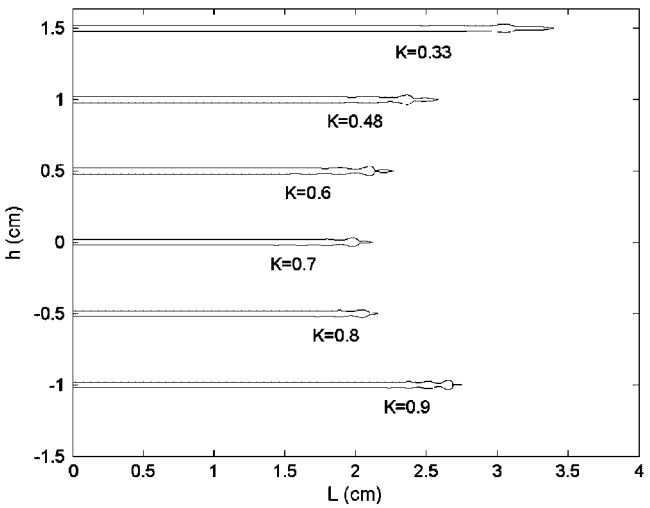

Figure 8. Calculated jet shapes of a jet perturbed at various wavenumbers.

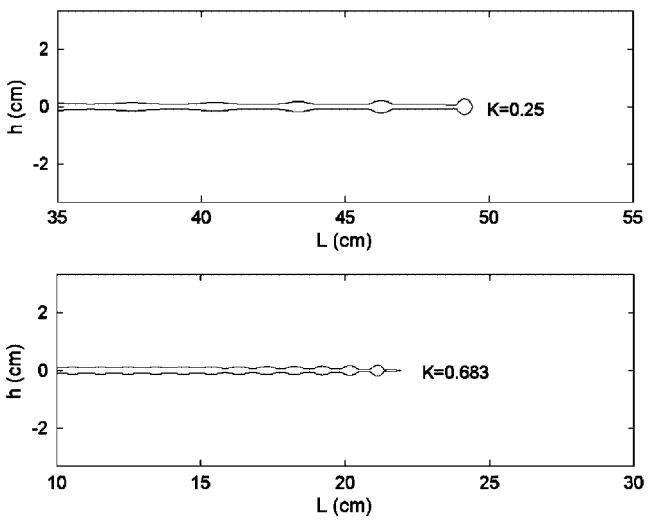

Figure 9. Numerical simulations of the experimental cases of Rutland and Jameson [34].

to a spectrum of disturbance of the Fourier form, but to suffer disruption under the action of the disturbance with the largest growth rate. Figure 10 shows the present predictions of water jets of $d = 0.4$ mm issuing at various jet velocities, namely $U = 1.25$, 1.37, 1.50, 1.57, and 1.72 m/s. In the analysis, these jets were assumed to be perturbed by a disturbance of $K = 0.7$, which should grow the fastest. From Figure 10, it can be clearly seen that the changes of the velocity apparently do not affect the sizes of main and satellite drops. The results show that the break-up length increases with the jet velocity, and the relationship between them is basically linear.

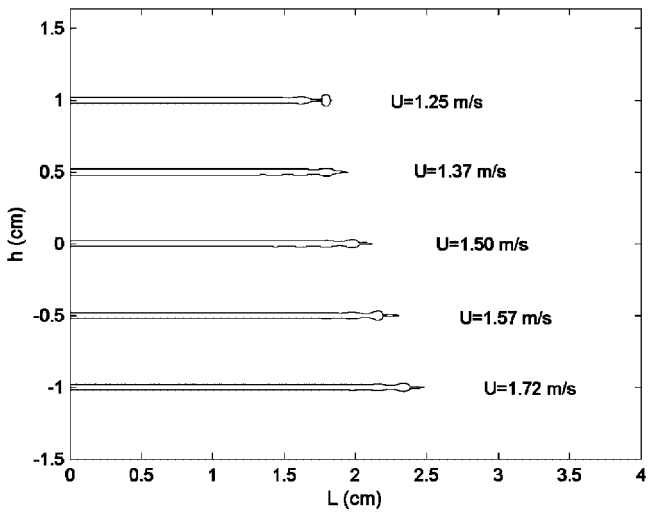

Figure 10. Numerical simulations of water jets issuing at various velocities.

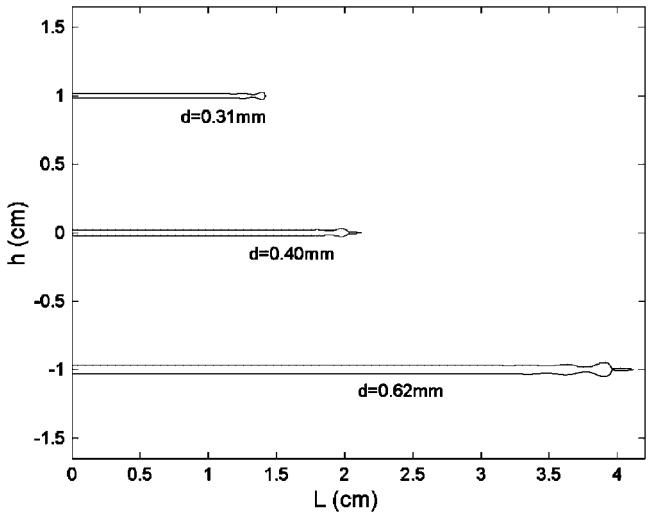

Figure 11. Numerical simulations of water jets issuing from various nozzles.

Besides the velocity, the jet diameter is also an essential factor to affect the jet behaviour. Figure 11 shows the effects of the diameter on drop size and break-up length using the case of $U = 1.5\,\mathrm{m/s}$ in Figure 10, but with three different diameters of $d = 0.31,\ 0.40,\ 0.62\,\mathrm{mm}$. It is obvious that the larger the jet diameter is, the bigger the drops are produced, as shown in Figure 11. Meanwhile, the break-up length also increases nonlinearly with increasing the diameter size of the jet. Furthermore, the values of L/d for the cases of $d = 0.31,\ 0.40,\ 0.62\,\mathrm{mm}$ (i.e. 45.56, 53.04, and 66.50, respectively) are nonlinearly proportional to the Weber

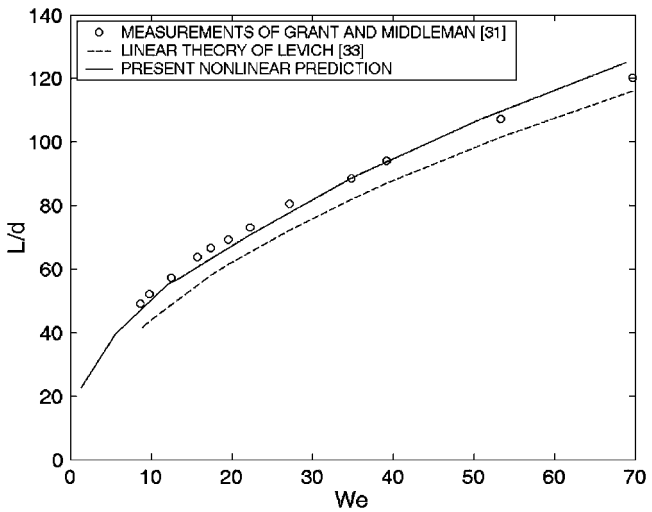

Figure 12. Variations of normalized break-up length with Weber number.

numbers of these cases (i.e. 9.795, 12.64, and 19.59, respectively). Note that the definition of the Weber number is $We = \rho d U^2/\sigma$.

Among a spectrum of disturbance, the most unstable wave corresponding to $K = 0.7$ should first satisfies the break-up condition. Figure 12 shows that the present prediction for the break-up lengths of capillary jets subjected to a disturbance of $K = 0.7$ was compared to experimental work of Grant and Middleman [31], which is an empirical correlation of five different liquid jets with a variety of diameters. The linear theory of Levich [33] was also applied to predict the jet break-up length. As shown in Figure 12, the curve of the present prediction appears nonlinear in the range of Weber number from 0 to 40 while it becomes approximately linear for higher Weber numbers. Note that the nonlinear behaviour of the break-up length for lower Weber numbers is similar to the results of the cases in Figure 11. The prediction of the linear theory of Levich [33] exhibits the similar behaviour along the curve, but it is underestimated. Based on the same flow conditions, the curve predicted by the present nonlinear model shows a better agreement with the measurements than the linear analysis. The reason for this may be that the present simulation can account for the existence of all harmonics and their growth variations.

7. GROWTH RATE OF SURFACE WAVE

The variations of logarithmic value of the wave amplitude predicted by the linear theory of Rayleigh [8] and the nonlinear theory of Yuen [15] were linear with time. In other words, the wave growth rates for the fundamental and harmonics modes were all assumed to be constant in their analyses. In fact, it has been observed by Goedde and Yuen [35] that for an actual liquid jet the surface growth at each location along the wavelength is different and varies with time. Goedde and Yuen [35] also plotted the logarithmic value of the difference between the amplitude at the swell and that at the neck, and then used the linear region on the curve to

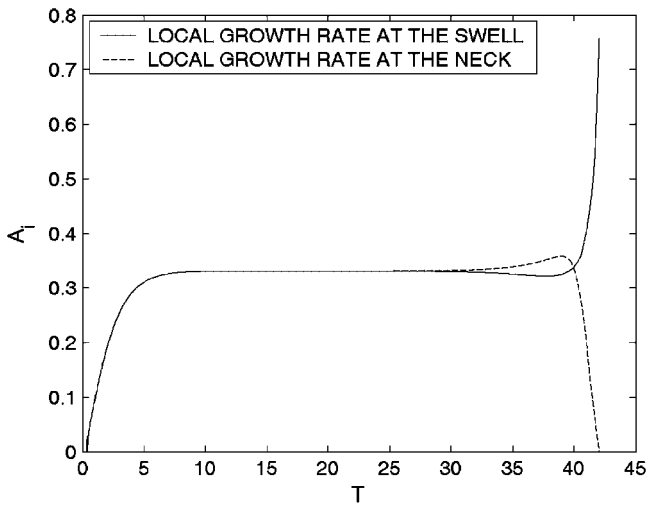

Figure 13. Variations of local growth rate with time.

describe the growth rate. Later, Ashgriz and Mashayek [36] utilized the similar time-averaging process to examine the temporal growth of the disturbances on viscous jet surface. However, it should be pointed out that a single, time-averaging growth rate does not properly describe the actual behaviour of the jet.

Therefore, a formulation for the instantaneous growth rate at any location along the wavelength is proposed in the present study as follows:

$$A_i = \frac{\ln(\xi_i^{K+1}/\xi_i^K)}{T^{K+1} - T^K} \tag{23}$$

where ξ_i is the dimensionless amplitude of the disturbance at t he location i along the wavelength and A_i represents the instantaneous, local growth rate. Figure 13 presents the variations of the local growth rates at the swell and neck points with time for the disturbance of $K = 0.7$. For this case, the growth rates at both locations increase quickly from $T = 0$ to 10, and then they keeps almost constant until the jet is about to break up. It is interesting that the experimental work of Goedde and Yuen [35] showed the similar results. They reported that the logarithmic value of the difference between the amplitude at the swell and that at the neck varies linearly except close to the break-up time. As seen in Figure 13, the present analysis demonstrates that the growth rate of the swell increases suddenly and rapidly, but, on the contrary, the neck stops to grow just before main and satellite drops are detached from the jet.

In order to compare the present results with other data in the previous literatures, an average value of the constant regions on the curves in Figure 13 was adopted to represent the global growth rate of the disturbance, even though it is not proper to describe the instability of the jet with an average growth rate. Figure 14 shows the global growth rate A as a function of wavenumber K; for the comparison, the experimental results of Donnely and Glaberson [32] and the linear solutions of Rayleigh [8] are also shown. These results show that for the long waves ($K < 1$) the growth rate is positive, and hence the long waves can grow;

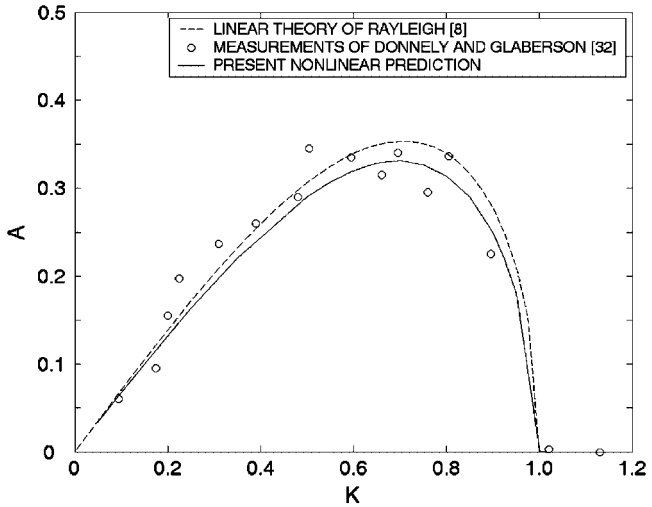

Figure 14. Variations of global growth rate with wavenumber.

for the short waves ($K > 1$), the growth rate is zero, and therefore the shore waves do not grow. As shown in Figure 14, the present nonlinear model predicts slightly lower growth rates than those obtained from the dispersion equation of Rayleigh [8] though both predictions are in agreement with the measurements. For $K > 0.6$, the present nonlinear predictions basically agree better with the measurements than the solutions of the linear theory do.

8. CONCLUSIONS

Major conclusions of the present study can be summarized as follows.

1. The sizes of main and satellite drops produced from capillary jets basically increase with increasing disturbance wavelength or nozzle diameter. The change of jet velocity apparently does not affect the sizes of the drops as long as the nozzle diameter keeps the same and the jet is perturbed at a fixed wavenumber.
2. The present results show that break-up length increases nonlinearly with increasing nozzle diameter. The results also confirm the Weber's linear relationship [9] between break-up length and jet velocity. However, when the break-up length is normalized by the nozzle diameter, the normalized break-up length appears nonlinear for low Weber numbers, and it gradually becomes linear as the Weber number increases.
3. In the comparison study, both linear and nonlinear predictions for break-up length are consistent with the distribution of experimental data, but the linear solutions are slightly underestimated. The reason for this may be attributed to the fact that the linear theory applies only the fundamental with a constant growth rate, but the present nonlinear simulation can account for the existence of all harmonics and their growth variations. However, a further study to validate this attribution is needed.

4. The global growth rates predicted by the present nonlinear model are slightly lower than those obtained from the dispersion equation of the linear theory. It is coincidental that a slower growth rate gives a longer jet break-up length. In fact, a single value of the global growth rate should not be used to describe the nonlinear behaviour of the jet. In the present study, local growth rates are computed, and the results show that the local growth rates for the swell and the neck increase with time at the early stage, and then they keep almost unvarying until the break-up occurs. Therefore, it is evident that the disturbance growth indeed varies temporarily though the wave grows steadily most of time.
5. The present computations show that the trough contracts at a slower rate than the swell grows for the case of long wavelength (e.g. $K = 0.3$). By contrast, the trough contracts at a faster rate than the swell grows for the case of short wavelength (e.g. $K = 0.7$ and 0.9). This phenomenon implies that the growth rate is also not constant in space so that local growth rates along the wavelength should be emphasized in the instability analysis of a capillary jet.

REFERENCES

1. Lefebvre AH. *Atomization and Sprays*. Hemisphere: New York, NY, 1989.
2. Lin SP, Reitz RD. Drop and spray formation from a liquid jet. *Annual of Review Fluid Mechanics* 1998; **30**: 85–105.
3. Lefebvre AH. *Gas Turbine Combustion*. Hemisphere: New York, NY, 1989.
4. Inamura T, Daikoku M. Numerical simulation of droplet formation from coaxial twin-fluid atomizer. *Atomization and Sprays* 2002; **12**:247–266.
5. Gooray A, Roller G, Galambos P, Zavadil K, Givler R, Peter F, Crowley J. Design of a MEMS ejector for printing applications. *Journal of Imaging Science and Technology* 2002; **46**:415–421.
6. Tseng FG, Kim CJ, Ho CM. *Microinjector Free of Satellite Drops and Characterization of the Ejected Droplets*, vol. 66. ASME, DSC Division MEMS (Publication): New York, 1998; 89–95.
7. Cheng S, Chandra S. A pneumatic droplet-on-demand generator. *Experiments of Fluids* 2003; **34**:755–762.
8. Rayleigh L. *Theory of Sound*. Macmillan: London, 1896 (Dover, New York, reprinted in 1945).
9. Weber C. Zum zerfall eines flussigkeitsstrahles (on the disruption of liquid jets). *Zeitschrift fur Angewandte Mathematik und Mechanik* 1931; **2**:136–141.
10. Sterling AH, Sleicher CA. The instability of capillary jets. *Journal of Fluid Mechanics* 1975; **68**:447–495.
11. Reitz RD, Bracco FV. Mechanism of atomization of a liquid jet. *Physics of Fluids* 1982; **25**:1730–1742.
12. Lin SP, Kang DJ. Atomization of a liquid jet. *Physics of Fluids* 1987; **30**:2000–2006.
13. Chuech SG, Przekwas AJ, Singhal AK. Numerical modeling for primary atomization of liquid jets. *AIAA Journal of Propulsion and Power* 1991; **7**:879–886.
14. Rutland DF, Jameson GJ. A non-linear effect in the capillary instability of liquid jets. *Journal of Fluid Mechanics* 1971; **46**:267–272.
15. Yuen MC. Non-linear capillary instability of a liquid jet. *Journal of Fluid Mechanics* 1968; **33**:151–163.
16. Lafrance P. Nonlinear breakup of a laminar liquid jet. *Physics of Fluids* 1975; **18**:428–432.
17. Chaudhar KC, Redekoff LG. The nonlinear capillary instability of a liquid jet: Part 1 theory. *Journal of Fluid Mechanics* 1980; **96**:257–274.
18. Bogy DB. Steady draw-down of a liquid jet under surface tension and gravity. *Journal of Fluid Mechanics* 1981; **105**:157–176.
19. Lee HC. Drop formation in a liquid jet. *IBM Journal of Research Development* 1974; **18**:364–369.
20. Torpey PA. A nonlinear theory for describing the propagation of disturbances on a capillary jet. *Physics of Fluids A* 1989; **1**:661–671.
21. Sellens RW. A one-dimensional numerical model of capillary instability. *Atomization and Sprays* 1992; **2**: 239–251.
22. Shokoohi F, Elrod HG. Numerical investigation of the disintegration of liquid jets. *Journal of Computational Physics* 1987; **71**:324–342.
23. Childs RE, Mansour NN. Simulation of fundamental atomization mechanism in fuel sprays. *AIAA 26th Aerospace Science Meeting* 1988, January 11–14, Reno, Nevada, Paper no. 88-0238.

24. Fromm JE. Numerical calculation of the fluid dynamics of drop-on-demand jets. *IBM Journal of Research Development* 1984; **28**:322–333.
25. Eggers J, Dupont TF. Drop formation in a one-dimensional approximation of the Navier–Stokes equation. *Journal of Fluid Mechanics* 1994; **262**:205–221.
26. Eggers J. Nonlinear dynamics and breakup of free-surface flows. *Reviews of Modern Physics* 1997; **69**:865–929.
27. Brenner MP, Eggers J, Joseph K, Nagel SR, Shi XD. Breakdown of scaling in droplet fission at high Reynolds number. *Physics of Fluids* 1997; **9**:1573–1590.
28. Wilkes ED, Phillips SD, Basaran OA. Computational and experimental analysis of dynamics of drop formation. *Physics of Fluids* 1999; **11**:3577–3598.
29. Ambravaneswaran B, Wilkes ED, Basaran OA. Drop formation from a capillary tube: comparison of one-dimensional and two-dimensional analyses and occurrence of satellite drops. *Physics of Fluids* 2002; **14**: 2606–2621.
30. Anderson JD. *Computational Fluid Dynamics*. McGraw-Hill: New York, NY, 1995.
31. Grant RP, Middleman S. Newtonian jet stability. *AIChE Journal* 1966; **12**:669–678.
32. Donnely RJ, Glaberson W. Experiment on the capillary instability of a liquid jet. *Proceedings of the Royal Society of London*, *Series A* 1965; **290**:547–556.
33. Levich VG. *Physicochemical Hydrodynamics*. Prentice-Hall: New Jersey, NJ, 1962.
34. Rutland DF, Jameson GJ. Theoretical prediction of the sizes of drops formed in the breakup of capillary jets. *Chemical Engineering Science* 1970; **25**:1689–1968.
35. Goedde EF, Yuen MC. Experiments on liquid jet instability. *Journal of Fluid Mechanics* 1970; **40**:495–511.
36. Ashgriz N, Mashayek F. Temporal analysis of capillary jet breakup. *Journal of Fluid Mechanics* 1995; **291**: 163–190.

